



Funded by the Seventh Framework
Programme of the European Union



Project full title:

Hepatic and Cardiac Toxicity Systems modelling

Project acronym:

HeCaToS

Collaborative project

HEALTH.2013.1.3.-1:

Modelling toxic response in case studies for predictive human safety assessment

FP7-HEALTH-2013-INNOVATION-1-602156-HeCaTos

Deliverable Report D1.2:

**Report on predictions for small molecule passive membrane transfer
of known toxicants and their metabolites using MD**

Work package 1

Due date of deliverable: M36

Actual submission date: October 2016, M37

Start date of project: October, 2013

Duration: 60 months

Maastricht University (UM)

Project co-funded by the European Commission within the 7th Framework Programme (2013-2018)		
Dissemination Level		
PU	Public	X
PP	Restricted to other programme participants (including the Commission Services)	
RE	Restricted to a group specified by the consortium (including the Commission Services)	
CO	Confidential, only for members of the consortium (including the Commission Services)	

Contributions to deliverable - Internal review procedure

Deliverable produced by:	Date:
Ian R Gould - Partner ICL-ICB	October 2016
Matt Segall - Partner Optibrium	October 2016
Deliverable internally reviewed by:	Date:
Jos Kleinjans - Partner UM	October 2016

Contents

Publishable Summary.....	3
Objectives	4
Introduction	5
Results.....	6
Self-Assembly Simulations	6
Translocation of BODIPY molecular rotors comparison with experiment.....	9
SEP Inhibitor modelling.....	10
Anthracycline Parameterization and Validation	13
Difficulties	14
References	14

PUBLISHABLE SUMMARY

We have applied our Lipid 14 force field [1] to investigate the process of small molecule translocation in model lipid bilayers. This work has necessitated a degree of methodological validation of the force field through the simulation of the self-assembly process of lipid bilayers which has resulted in the publication of two papers [2,3]. Figure 1. below illustrates the fundamental processes of self-assembly of bilayers.

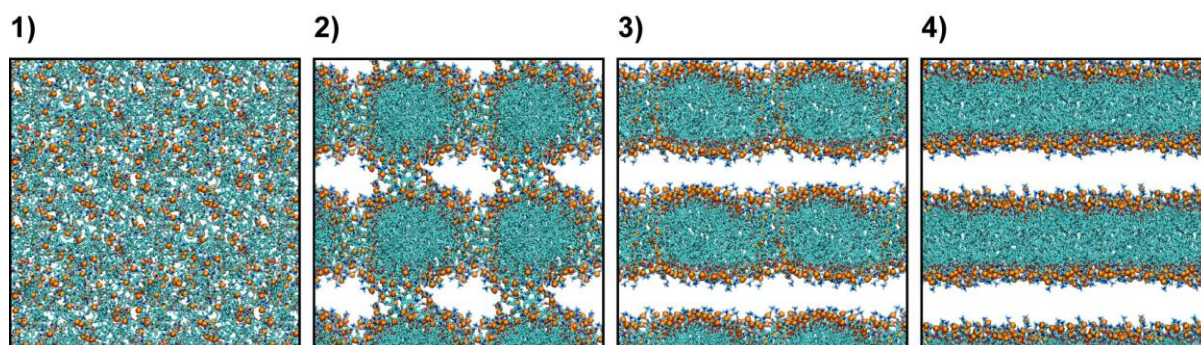


Figure 1: General mechanism of the all-atom bilayer self-assembly. Representative snapshots from one of the DOPC simulations illustrate four characteristic stages in the self-assembly process. The phospholipids are represented as stick models, with the head group phosphorus atoms highlighted as orange spheres. For clarity, water, ions and hydrogens are not shown. Note that each snapshot not only includes the primary simulation box, but also portions of surrounding periodic images.

Subsequent to the successful validation of our underlying force field we have advanced to investigating the translocation of a series of BODIPY based molecular rotors in different lipid bilayers, DOPC and DPPC, which we have been able to successfully interpret and corroborate through fluorescence lifetime spectroscopy; this work has been published [4,5].

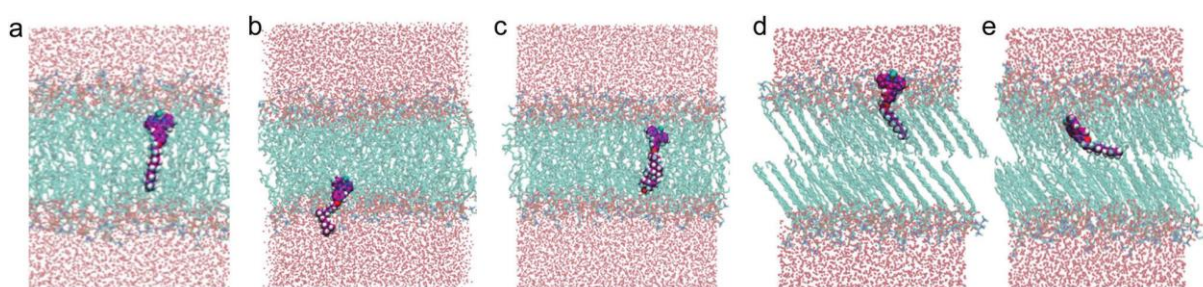


Figure 2: Molecular dynamics simulations showing the orientations of (a) rotor 1, (b) rotor 2, and (c) rotor 3 in a DOPC bilayer, and (d) and (e) the two orientations of rotor 1 in a gel phase DPPC bilayer. Simulated DOPC bilayers have a membrane thickness of 37.0 ± 0.2 Å and DPPC bilayers have a membrane thickness of 37.9 ± 0.5 Å.

The published work has constructed the framework from which we have been able to investigate the mechanism of translocation of a series of human bile salt export pump (BSEP) inhibitors; it has been suggested that inhibition of BSEP activity by drugs could be one of the mechanisms that initiate human DILI. We have identified a set of 12 matched molecular pairs exhibiting unexpected activity profiles and have applied our MD methodology to discern their behavior in two different lipid bilayers [6]. We have discerned that for a passive model of translocation there is a very high level of correlation between the permeation time and IC₅₀ value of the molecule, which is consistent for both lipids. This work is currently being written up for publication.

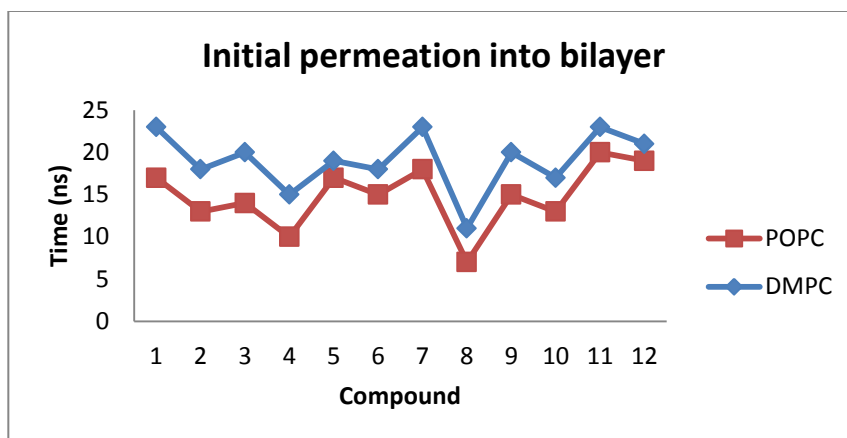


Figure 3: Rates of permeation into bilayer for the 12 matched molecular pairs.

We are currently investigating the process of translocation for these molecules through the application of our recently implemented Potential of Mean Force (PMF) code, which allows for a more rigorous thermodynamic interpretation of the process of insertion. This work is almost complete and will lead to a publication.

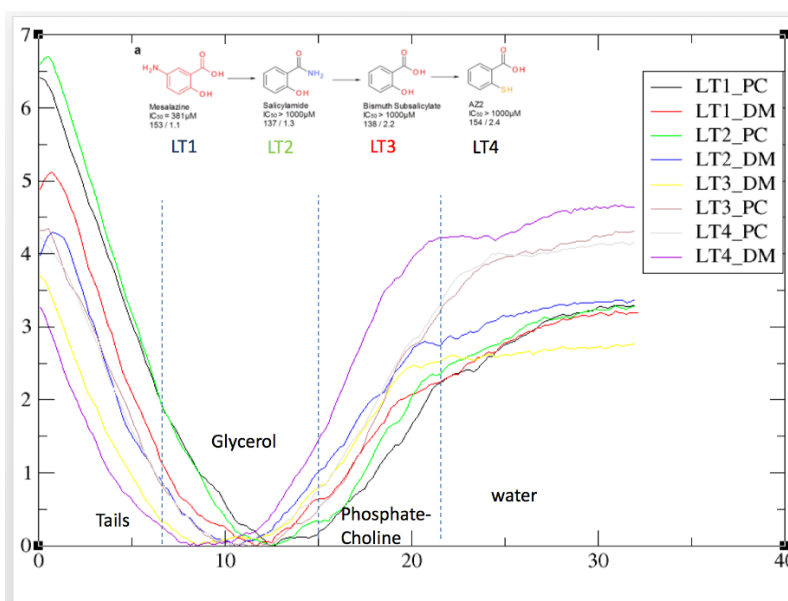


Figure 4: PMF profiles of insertion of the first four ligands in two different lipids, POPC AND DMPC.

We have parameterized the Anthracyclines, Doxorubicin, Daunorubicin, Idarubicin and Epirubicin for AMBER and so their interaction with lipid bilayers or with identified protein targets can be explored. From the parameterization process we have a large amount of quantum mechanically derived data which can be compared with experiment and this will form the basis of a publication.

OBJECTIVES

- To model the translocation of small ligands (toxicants) through model membrane bilayers to determine if correlation with molecular properties, such as diffusion rate and position in the bilayer, could rationalise the efficacy/toxic capacity of the ligand;
- Creation of MD protocols, techniques and analysis tools to implement and apply this methodology.

INTRODUCTION

Membranes are integral components of the cell, separating intracellular compartments from the cytosol. Such membranes consist of a back-to-back arrangement of lipid molecules, driven into a bilayer structure by the hydrophobic effect, leaving the polar lipid head groups exposed to water, and bringing the nonpolar lipid tail groups together. The composition of cell membranes is complex, with constituent species including, but not limited to, saturated and unsaturated PC and PE lipids, sphingomyelin and cholesterol, which serve as a matrix in which membrane proteins may reside [7]. Cell membranes possess functions such as regulating transport in to and out of the cell and modulating the activity of membrane embedded ion channels and proteins [8,9].

In order to probe the many roles of membranes in the cell, membrane structures are studied experimentally using techniques such as X-ray and neutron scattering, IR/Raman, and NMR spectroscopy [10,11]. To gain atomic-level resolution, however, membranes may also be simulated computationally using molecular dynamics (MD). The validity of results obtained using MD methods depends, to a large extent, on the potential energy function, or force field, that is used. Membranes can be simulated using all-atom, united-atom, or coarse-grained models [12–19] with the increasing simplicity of each representation allowing access to larger models and longer time scales, at the expense of atomic detail. All-atom models may be preferred for bilayer simulations due to their ability to reproduce NMR order parameters and easy combination with all-atom protein, nucleic acid, carbohydrate, and small molecule force fields [20–22].

Translocation of small ligands across the cell membrane are of inherent interest in trying to rationalise their potential toxic effects. To facilitate a molecular understanding of the mechanism of transport and therefore interactions with the lipid bilayer MD simulation protocols and parameters, for the ligands and lipids, need to be developed and applied. We have been developing over the past few years the necessary force fields [1] to address the MD modelling of membranes. This has led to the necessity to validate such force fields in respect of their ability to reproduce known experimental data before they can be applied to a wider variety of problems with a significant degree of confidence.

One of the most stringent tests that can be applied to all atom simulation of lipid bilayers is to assess whether the force field capable of correctly producing self-assembled bilayers from completely randomized homogenous mixtures of lipid and water. It should be noted that this has never been attempted or achieved at the all atom level of simulation. This test is one of the first investigations we have undertaken to determine the validity of the Lipid 14 [1] force field; we have shown that for symmetric zwitter-ionic and anionic lipid systems we are capable of reproducing the experimentally determined bilayers [2,3].

One of the main parameters controlling the rate of diffusion of molecules in membranes is the viscosity of the surrounding environment, so precise measurements of intracellular viscosity are necessary in order to fully understand the dynamics of reactions within a cell [23]. This is particularly true within membrane systems, where viscosity and the subsequent lipid diffusion dynamics play a vital role in the activity of the membrane [24]. Therefore, to assess the ability of our modelling of small ligands in lipid bilayers we have identified a series of boron-dipyrromethene (BODIPY) based molecular rotors which we have simulated in two different bilayers, dioleoyl-phosphatidylcholine (DOPC) and dipalmitoyl phosphatidylcholine (DPPC). For these ligands it is necessary to parameterize them using the general AMBER force field (GAFF) [22] which provides a robust test of the methodology that will be applied for subsequent ligand parameterization. The results of these simulations has been published in collaboration with experimental validation [4,5].

Having determined the methodological basis and validation of the pipeline for performing MD simulations of lipid bilayers and their interaction with small ligands, the next step is the investigation of a series of small ligands for which there is experimental data. We have chosen to investigate the mechanism of translocation of a series of human bile salt export pump (BSEP) inhibitors, it has been suggested that inhibition of BSEP activity by drugs could be one of the mechanisms that initiate human drug-induced liver injury (DILI). We have identified a set of 12 matched molecular pairs exhibiting unexpected activity profiles and have applied our MD methodology to discern their behavior in two different lipid bilayers [6]. We have discovered that there is a strong correlation between the passive diffusion time of the ligands and their corresponding IC_{50} values, the 12 ligands were chosen explicitly as other *in silico* predictors could not correctly correlate with the IC_{50} 's. This work will be written up shortly for publication in a peer reviewed journal.

The passive diffusion model that we have applied to the BSEP inhibitors is amenable to analysis in respect of the permeation time taken and to analysis of the orientation of the molecules in the bilayer. However, this type of methodology does not impart any energetic information on the barriers to insertion or translocation across the membrane. We have recently implemented the Potential of Mean Force (PMF) method within the GPU version of our AMBER MD code. This facilitates the capability to interrogate the energetic profile of a ligand as it is “pulled” through the bilayer. We are performing these simulations in the same two different lipid bilayers as for the passive modelling. These are ongoing and we will be analyzing and publishing the results in due course.

From the set of reference drugs in the MS 5 reference compound library we have focused upon the Anthracyclines, Doxorubicin, Epirubicin, Daunorubicin and Idarubicin, which are key HeCaToS compounds [25]. We have parametrised these for use in AMBER and so they can be simulated in lipid environments or with identified proteins.

RESULTS

Self-Assembly Simulations

The simulation of the self-assembly of lipid bilayers, both zwitter-ionic and anionic, at the all atom level of description is a World's first [2,3]. The impact of these papers is extremely high, paper [2] published in chem comm in 2015 has 7 citations, and paper [3] published in 2016 has an Altmetrics score of 2.

The subsequent figures and tables highlight both the mechanism of self-assembly and the high level of correlation between the simulated and experimentally determined properties. Figure 2, is extremely pertinent as it illustrates the level of agreement in respect to the dynamical properties of the lipids through comparison with NMR order parameters.

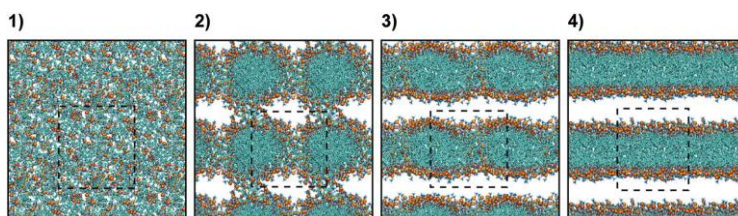


Figure 1: General mechanism of the all-atom bilayer self-assembly. Four characteristic stages were observed during the self-assembly process and are illustrated here by representative snapshots from one of the simulations. Phospholipids are shown as stick models, with the phosphorus atoms in the constituent head groups represented as orange spheres. Water, ions and hydrogens have been omitted for clarity. Please note that the snapshots include portions of neighbouring periodic images in addition to the simulation unit cell, which is indicated by dashed-lined squares.

Table 1: Simulation system details

System	Number of lipids	TIP3P water/lipid ratio	Number of K ⁺ /Cl ⁻	Number of Na ⁺	Simulation time per repeat ^a (ns)	Simulation temperature (K)
DOPC ^b	128	32.8	12/12	—	1000	303.0
POPC	128	31.0	11/11	—	1000	303.0
POPE	128	32.0	12/12	—	1000	310.0
DPPC ^b	128	30.1	11/11	—	1000	323.0
POPS	128	50	—	128	1000	303.0
POPG	128	50	—	128	1000	303.0
DOPS	128	50	—	128	1000	303.0
DOPG	128	50	—	128	1000	303.0

^a For each of the three lipid force fields – Lipid14, Charmm C36 and Slipids – three simulation repeats of 1 μ s duration each were run on each system. ^b Three additional 1 μ s repeats were performed for the C36 DPPC and the C36 DOPC systems using a van der Waals force switch function over 8 to 12 Å (all other simulations were run with a strict 10 Å cut-off).

Table 2: (a) Formation time, number of lipids per leaflet and volume per lipid for self-assembled bilayers. (b) thickness and isothermal compressibility moduli for the self-assembled bilayers

(a)																			
Lipid	Sim. no.	Bilayer formation time ^a (ns)				No. of lipids per leaflet				Area per lipid ^d (Å ²)				Volume per lipid ^d (Å ³)					
		C36 ^b		Slipids ^c	Lipid14	C36		Slipids	Lipid14	C36		Slipids	Exp.	C36		Slipids	Exp.		
		cut	fsw			cut	fsw			cut	fsw			cut	fsw				
DOPC	1	150	135	152	246	66/62	61/67	64/64	65/63	69.3 ± 1.2	67.8 ± 1.2	69.1 ± 1.1	69.1 ± 1.0	67.4 ³⁹ 72.5 ⁴⁴	1251.5 ± 4.4	1238.1 ± 4.2	1280.9 ± 4.8	1271.7 ± 4.4	1303 ⁴⁴
	2	285	145	385	717	62/66	67/61	64/64	64/64	69.2 ± 1.1	67.8 ± 1.1	69.0 ± 1.1	69.2 ± 1.1	1251.5 ± 4.4	1238.1 ± 4.2	1280.9 ± 4.7	1271.6 ± 4.4		
	3	720	160	—	941	63/65	65/63	—	61/67	69.0 ± 1.2	67.6 ± 1.1	—	69.7 ± 1.0	1251.3 ± 4.4	1238.1 ± 4.2	—	1271.7 ± 4.5		
POPC	1	375	160	94	64/64	66/62	—	63/65	65.5 ± 1.2	63.8 ± 1.2	—	66.5 ± 1.1	64.3 ⁴⁰ 68.3 ⁴¹	1207.3 ± 4.3	1191.9 ± 4.2	—	1224.8 ± 4.3	1256 ⁴¹	
	2	535	325	228	63/65	66/62	67/61	62/66	65.7 ± 1.3	63.7 ± 1.2	—	66.6 ± 1.1	—	1207.4 ± 4.3	1191.7 ± 4.2	—	1224.7 ± 4.4		
	3	755	425	—	68/60	62/66	—	—	65.6 ± 1.3	63.8 ± 1.1	—	—	—	1207.1 ± 4.4	1191.9 ± 4.1	—	—		
POPE	1	70	95	89	62/66	61/67	—	69/59	56.0 ± 1.1	56.9 ± 1.1	—	60.7 ± 1.0	56.6 ⁴⁹ 58.4 ⁴³ 59–60 ⁵⁰	1141.1 ± 4.4	1134.9 ± 4.3	—	1171.5 ± 4.5	1175.1 ⁴³ 1180 ⁵⁰	
	2	100	115	153	63/65	62/66	58/70	63/65	56.3 ± 1.1	56.5 ± 1.1	—	60.8 ± 1.0	—	1141.2 ± 4.5	1134.7 ± 4.5	—	1171.3 ± 4.5		
	3	125	205	245	71/57	67/61	63/65	—	57.2 ± 1.3	56.9 ± 1.1	—	59.8 ± 1.1	—	1140.4 ± 4.8	1135.1 ± 4.3	—	1171.4 ± 4.5		
DPPC	1	230	35	89	75	65/63	66/62	64/64	62/66	62.2 ± 1.4	54.4 ± 0.6	62.3 ± 1.2	65.0 ± 1.1	63.1 ⁴⁰ 64.3 ⁴²	1178.8 ± 5.1	1099.6 ± 4.6	1203.2 ± 5.2	1196.1 ± 4.6	1232 ⁴⁴
	2	350	85	117	157	64/64	64/64	63/65	66/62	62.3 ± 1.3	52.2 ± 0.6	62.4 ± 1.3	65.0 ± 1.1	1179.4 ± 4.9	1098.8 ± 4.6	1203.3 ± 5.3	1196.2 ± 4.6		
	3	440	325	123	302	60/68	62/66	63/65	63/65	62.3 ± 1.4	54.8 ± 0.7	62.2 ± 1.2	64.7 ± 1.2	1178.7 ± 5.0	1102.6 ± 4.6	1203.1 ± 5.2	1196.1 ± 4.6		
POPS	1	70	136	N/A	64/64	68/60	—	N/A	58.2 ± 1.2	57.5 ± 1.2	—	N/A	62.7 ⁴⁵	1147.1 ± 4.8	1120.5 ± 4.8	—	N/A	1198.5 ⁴⁵	
	2	84	156	N/A	63/65	63/65	—	N/A	58.4 ± 1.4	57.7 ± 1.3	—	N/A	—	1147.2 ± 4.7	1121.6 ± 4.7	—	N/A		
	3	160	—	N/A	62/66	—	—	N/A	58.1 ± 1.1	—	—	N/A	—	1146.9 ± 4.8	—	—	N/A		
POPG	1	47	106	90	64/64	61/67	—	66/62	66.7 ± 1.3	67.2 ± 1.4	—	68.9 ± 1.3	64.3 ⁴⁷ 66.1 ⁴⁶	1163.9 ± 4.7	1151.0 ± 4.6	—	1192.6 ± 4.8	1208.7 ⁴⁶	
	2	106	330	133	64/64	64/64	64/64	66.7 ± 1.3	67.4 ± 1.3	—	—	68.8 ± 1.3	—	1164.1 ± 4.8	1151.2 ± 4.6	—	1192.5 ± 4.8		
	3	155	350	856	62/66	62/66	65/63	66.8 ± 1.3	67.3 ± 1.6	—	—	68.7 ± 1.3	—	1163.9 ± 4.7	1151.0 ± 4.6	—	1192.5 ± 4.8		
DOPS	1	46	79	98	65/63	65/63	61/67	63.7 ± 1.0	63.1 ± 1.3	—	—	66.3 ± 1.1	64.1 ⁴⁸	1191.0 ± 4.7	1170.6 ± 4.6	—	1229.1 ± 4.9	1228 ⁴⁸	
	2	53	127	99	69/59	63/65	62/66	64.3 ± 1.2	63.3 ± 1.2	—	—	65.8 ± 1.2	—	1191.0 ± 4.8	1170.8 ± 4.6	—	1229.1 ± 4.9		
	3	68	242	107	67/61	65/63	67/61	63.9 ± 1.1	62.8 ± 1.2	—	—	65.9 ± 1.2	—	1191.0 ± 4.7	1170.7 ± 4.6	—	1229.2 ± 4.9		
DOPG	1	63	251	86	67/61	62/66	64/64	70.6 ± 1.2	71.2 ± 1.3	—	—	71.8 ± 1.2	69.1 ⁴⁷ 70.8 ⁴⁶	1206.7 ± 4.8	1198.4 ± 4.6	—	1238.6 ± 4.9	1265 ⁴⁶	
	2	66	323	90	65/63	62/66	63/65	70.5 ± 1.3	70.9 ± 1.2	—	—	71.6 ± 1.2	—	1206.8 ± 4.8	1198.3 ± 4.5	—	1238.5 ± 4.9		
	3	202	448	326	62/66	65/63	67/61	70.6 ± 1.3	71.0 ± 1.4	—	—	72.0 ± 1.2	—	1206.8 ± 4.8	1198.4 ± 4.6	—	1238.6 ± 4.9		

(b)																
Lipid	Sim. no. ^e	Bilayer thickness D_{HH} ^b (Å)					Luzzati thickness D_L ^b (Å)					Isothermal compressibility modulus K_A ^b (mN m ⁻¹)				
		C36 ^f					C36 ^f					C36 ^f				
		Lipid14	cut	fsw	Slipids ^g	Exp.	Lipid14	cut	fsw	Slipids ^g	Exp.	Lipid14	cut	fsw	Slipids ^g	Exp.
DOPC	1					35.3, ⁵³ 36.7, ³⁹					35.9, ⁴⁴ 36.1, ⁵²					265, ⁵⁷ 300, ⁵⁶
	2	37.3 ± 0.3	37.9 ± 0.4	38.1 ± 0.2	36.0 ± 0.4	36.9, ⁴¹ 37.1 ⁵²	36.2 ± 0.1	36.6 ± 0.1	37.1 ± 0.0	36.7 ± 0.2	38.7 ⁴⁹	320 ± 30	350 ± 10	370 ± 40	430 ± 40	318 ⁵⁵
	3															
POPC	1										36.8, ⁴¹ 39.1 ⁴⁰					
	2	37.3 ± 0.0	38.3 ± 0.3		36.3 ± 0.4	37 ⁴¹	36.8 ± 0.1	37.4 ± 0.0		36.8 ± 0.0	39.1 ⁴⁰	270 ± 30	300 ± 20		360 ± 40	180–330 ⁵⁴
	3															
POPE	1															
	2	41.9 ± 0.4	41.1 ± 0.4		37.7 ± 0.5	39.5 ⁵⁰	40.4 ± 0.4	40.0 ± 0.2		38.8 ± 0.4	40.5 ⁴³	290 ± 40	310 ± 0		370 ± 10	233 ⁴⁹
	3															
DPPC	1															
	2	37.8 ± 0.1	43.8 ± 2.4	39.1 ± 0.4	36.2 ± 0.1	38, ³⁹ 38.3 ⁴⁴	37.9 ± 0.0	40.9 ± 1.0	38.6 ± 0.1	36.9 ± 0.1	39.0 ⁴⁰	230 ± 20	930 ± 30	290 ± 20	350 ± 20	231 ⁴⁴
	3															
POPS	1				N/A					N/A					N/A	—
	2	42.3 ± 0.1	42.4 ± 0.2		N/A	42.2 ⁴⁵	39.4 ± 0.1	39.0 ± 0.1		N/A	38.2 ⁴⁵	250 ± 50	250 ± 20		N/A	
	3				N/A					N/A					N/A	
POPG	1										36.6, ⁴⁶ 37.6 ⁴⁷					—
	2	36.8 ± 0.0	36.3 ± 0.0		34.8 ± 0.3	37.3 ⁵¹	34.9 ± 0.0	34.2 ± 0.0		34.7 ± 0.1	37.6 ⁴⁷	270 ± 10	220 ± 40		260 ± 10	
	3															
DOPS	1															—
	2	40.6 ± 0.1	41.3 ± 0.3		38.1 ± 0.1	39.0 ⁴⁸	37.3 ± 0.2	37.1 ± 0.1		37.3 ± 0.1	38.3 ⁴⁸	340 ± 40	270 ± 20		320 ± 10	
	3															
DOPG	1					—					35.7, ⁴⁶ 36.6 ⁴⁷					—
	2	36.3 ± 0.3	35.9 ± 0.1		34.6 ± 0.1		34.2 ± 0.0	33.8 ± 0.1		34.5 ± 0.1	36.6 ⁴⁷	290 ± 10	280 ± 40		320 ± 20	
	3															

^a Both the Lipid14, C36 and Slipids repeats for each lipid type are sorted in ascending order based on bilayer formation time. ^b cut refers to C36 simulations performed with a strict 10 Å cut-off, and fsw refers to C36 simulations run with a van der Waals force switch function over 8 to 12 Å. The lipids did not fully assemble into bilayers within 1 μs of simulation time in the last C36 DOPC fsw repeat and in the last C36 POPS cut-off repeat. ^c N/A refers to the fact that POPS is not included in the Slipids force field. The lipids did not fully assemble into bilayers within 1 μs of simulation time in the last Slipids POPC repeat. The last Slipids DOPC and POPG repeats were prolonged to 1100 ns and 1010 ns, respectively, in order to obtain at least 100 ns of simulation time for analysis of bilayer properties (see footnote d). ^d Areas and volumes per lipid are given as average ± standard deviation and were calculated from the interval from 50 ns after bilayer was fully formed until 1 μs of total simulation time. The exceptions are the three C36 DPPC repeats run with strict cut-off, for which analyses were done on the portion of each simulation where the overly ordered structure (described in the main text and visualized in Fig. S3, ESI) had been adopted. ^e Repeats listed in the same order as in (a). ^f cut refers to C36 simulations performed with a strict 10 Å cut-off, and fsw refers to C36 simulations run with a van der Waals force switch function over 8 to 12 Å. The lipids did not fully assemble into bilayers within 1 μs of simulation time in the last C36 DOPC fsw repeat and in the last C36 POPS cut-off repeat; these repeats are therefore not included in the relevant calculated averages. ^g N/A refers to the fact that POPS is not included in the Slipids force field. The lipids did not fully assemble into a bilayer within 1 μs of simulation time in the last Slipids POPC repeat; this repeat is therefore not included in the relevant calculated averages. The last Slipids DOPC and POPG repeats were prolonged to 1100 ns and 1010 ns, respectively, in order to obtain at least 100 ns of simulation time for the analysis of bilayer properties (see footnote h and (a)). ^h Properties given as the average across repeats ± standard deviation, where the average value from each individual repeat was calculated from the interval from 50 ns after bilayer was fully formed until 1 μs of total simulation time. The exceptions are the three C36 DPPC repeats run with strict cut-off, for which analyses were done on the portion of each simulation where the overly ordered structure (described in the main text and visualized in Fig. S3, ESI) had been adopted.

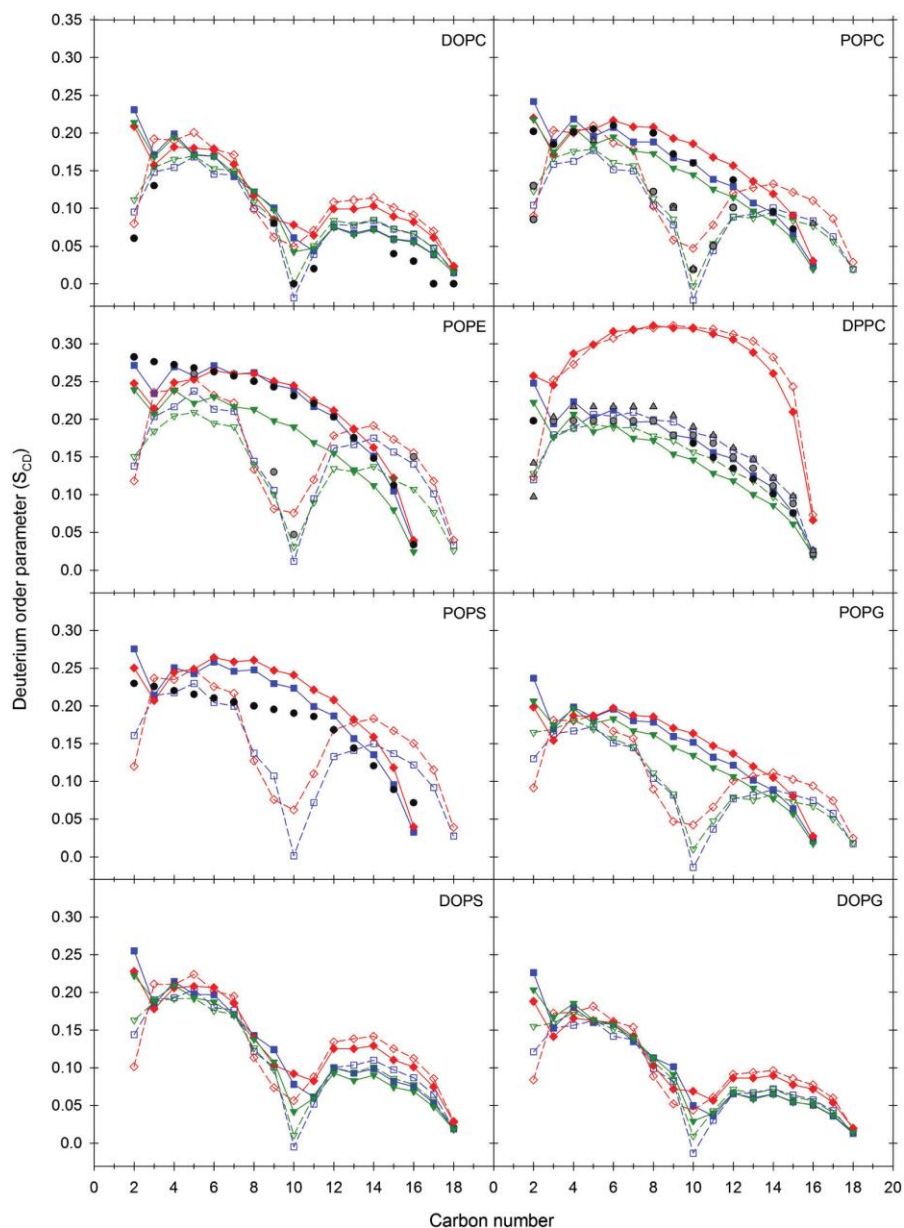


Figure 2: Deuterium order parameters (SCD) for self-assembled bilayers and comparison with experiment. Simulation values for each lipid/force field combination were calculated as averages across all repeats. The Lipid14 profiles are shown as blue squares, Charmm C36 (simulated with strict cut-off and denoted cut in Table 2a) and b) as red diamonds and Slipids as downward green triangles. The sn-1 acyl chain is indicated by filled symbols and solid lines, while sn-2 is represented by open symbols and dashed lines. For each repeat, the analysis was done on the interval from 50 ns after the bilayer was fully formed to the end of the simulation. Experimental data, where available, are given as black spheres for the sn-1 and gray spheres or upward triangles for the sn-2 acyl chain.

Translocation of BODIPY molecular rotors comparison with experiment

Validation of the quality of the lipid force field and the GAFF parameterized ligands is illustrated through the publications [4] and [5]. Reference [4] was published in PCCP in 2015 it has already accumulated 10 citations and an Altimetrics score of 4, reference [5] is only very recently published. Figure 3 illustrates the level of information that can be obtained from such simulations

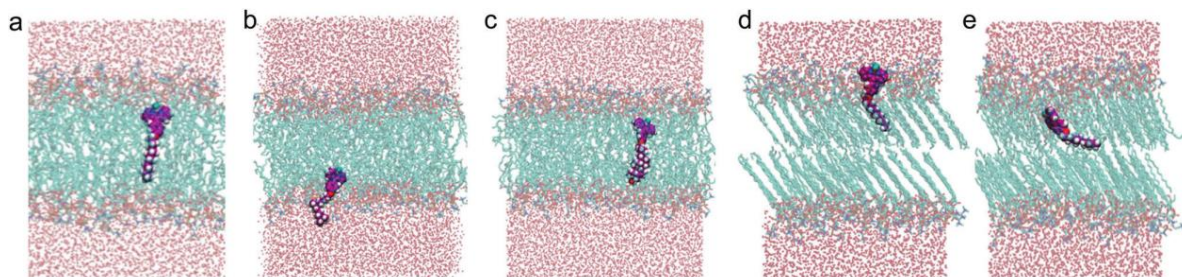


Figure 3: Molecular dynamics simulations showing the orientations of (a) rotor 1, (b) rotor 2, and (c) rotor 3 in a DOPC bilayer, and (d) and (e) the two orientations of rotor 1 in a gel phase DPPC bilayer. Simulated DOPC bilayers have a membrane thickness of 37.0 ± 0.2 Å and DPPC bilayers have a membrane thickness of 37.9 ± 0.5 Å.

Table 3 below illustrates the level of agreement that is obtained from the simulations and the fluorescence lifetime spectroscopy. This is a further validation of the applicability of both force fields developed and applied for small ligands in lipid bilayers.

Table 3: Diffusion coefficients calculated for the three rotors in DOPC bilayers using molecular dynamics simulations, FCS and the Saffman–Delbruck equation to calculate diffusion coefficients from the viscosity values calculated from the fluorescence lifetimes of the BODIP Y rotors.

Temperature/K	Diffusion coefficient/ $\mu\text{m}^2 \text{ s}^{-1}$								
	Rotor 1			Rotor 2			Rotor 3		
	Simulated	FCS	Lifetime	Simulated	FCS	Lifetime	Simulated	FCS	Lifetime
293	10.22	10.52	3.78	7.52	8.75	2.91	7.06	7.25	3.23
313	16.45	18.06	11.11	14.39	12.32	8.73	12.20	14.18	8.21
333	22.67	22.65	32.94	21.61	19.91	27.77	18.74	21.18	20.52

SEP Inhibitor modelling

We have chosen to study through the application of our modelling pipeline to 12 matched molecular pairs exhibiting unexpected activity profiles [6]. In Figure 4 below, the ligands are grouped in respect of their chemical composition. Group a) contains molecules with both carboxylic group, hydroxyl groups and in two cases primary amines; they are all small molecules of approx. MW 150 and all exhibit low calculated values of clogP. Group b) are composed of compounds of approx. MW 300, all have carboxylic acid moieties, a hydroxyl and a ketone oxygen; clogP values are all comparable between 4 and 5. Group c) consists of tertiary amines of approx. MW 270 and clogP values in the range of 3 to 4. The final group d) has only two members whose IC50 values differ by more than 3 orders of magnitude despite very similar composition and molecular properties.

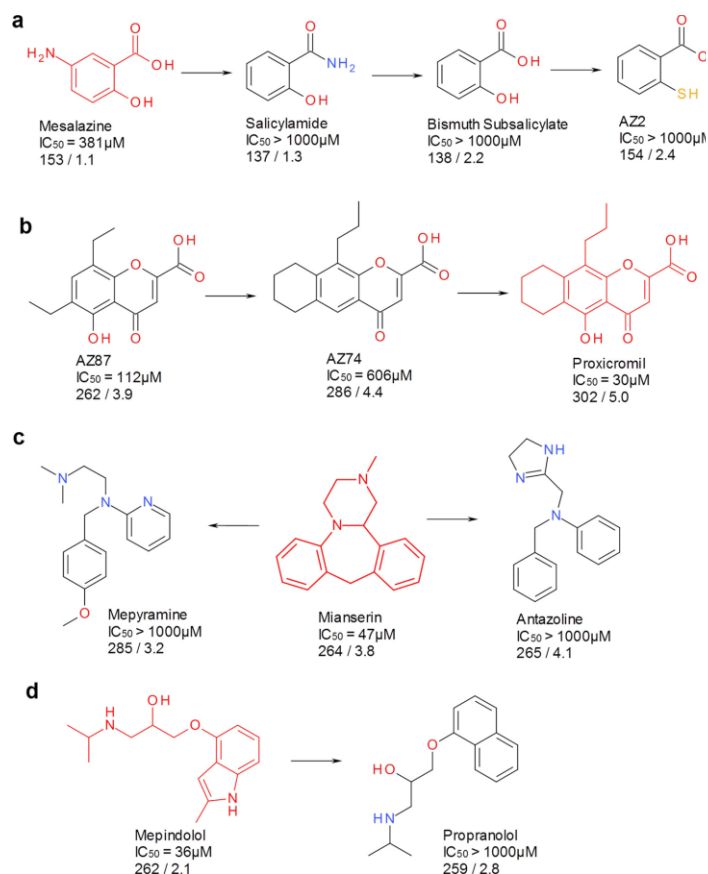


Figure 4: a–d, matched molecular pairs exhibiting unexpected activity profiles. Structures are displayed from left to right in order of increasing clogP. The molecular weight and calculated logP of each compound are expressed below the BSEP activities in the format molecular weight/clogP. The most potent BSEP inhibitor in each row is represented in red.

We have discovered that there is a clear correlation between the rate of permeation and the IC₅₀ Value. The choice of Lipid bilayer has not effect on the result.

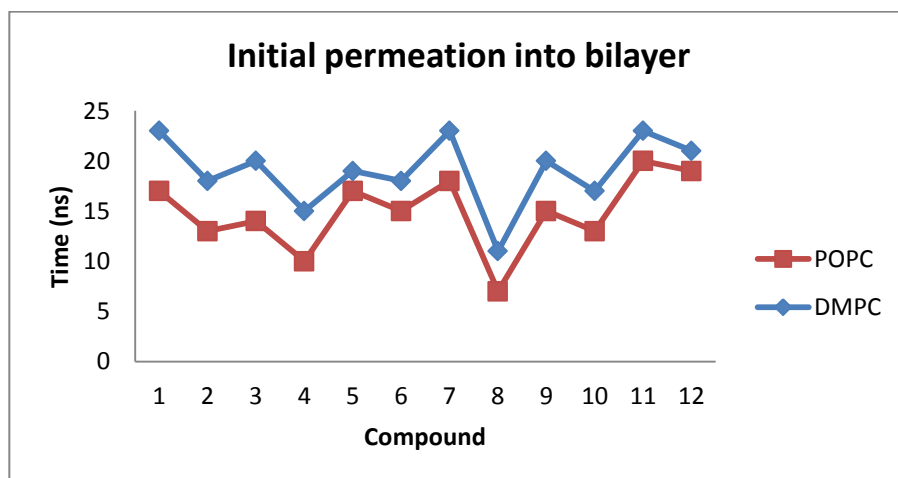


Figure 5: Rates of permeation into bilayer for the 12 matched molecular pairs. The numbering corresponds to group a) 1 to 4 from left to right b) 5 to 7 c) 8 to 10 and d) 11 to 12.

Whilst the rate of permeation is an interesting metric it does not impart any energetic information which can then be used in thermodynamic rationalization of the behavior of the ligands with the bilayer. We are, currently, investigating the thermodynamic profiles of inserting the ligands into the same lipid bilayers as for the passive diffusion model described above, this is being modelled by the application of the Potential of Mean Force (PMF) method. This is an extremely technically challenging method and has only recently been implemented in our MD GPU engine. As can be seen from Figure 6 below we have completed the study for group a) and are currently in the process of investigating group b), group c) and d) will be investigated shortly. Dr Toroz is currently in the process of writing a software suite to facilitate the detailed analysis of results from these simulations.

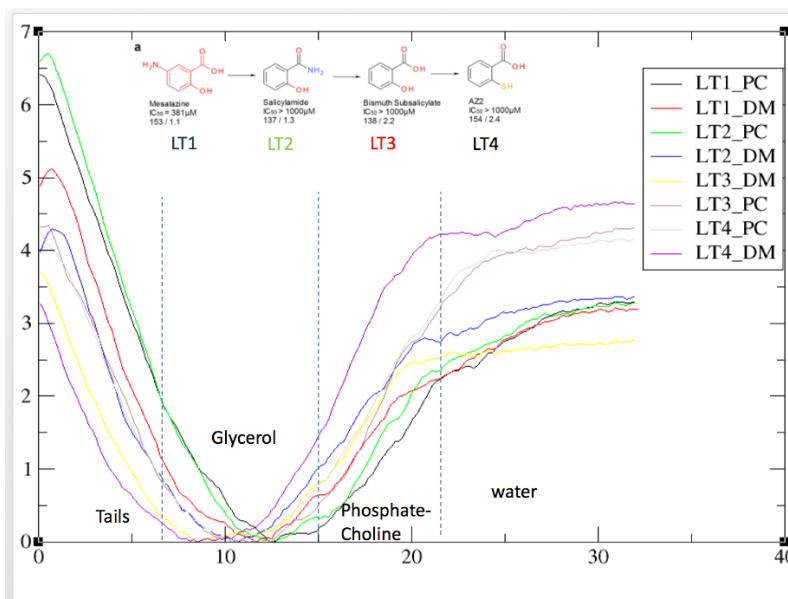


Figure 6: PMF profiles of insertion of group a) ligands in two different lipids, POPC and DMPC.

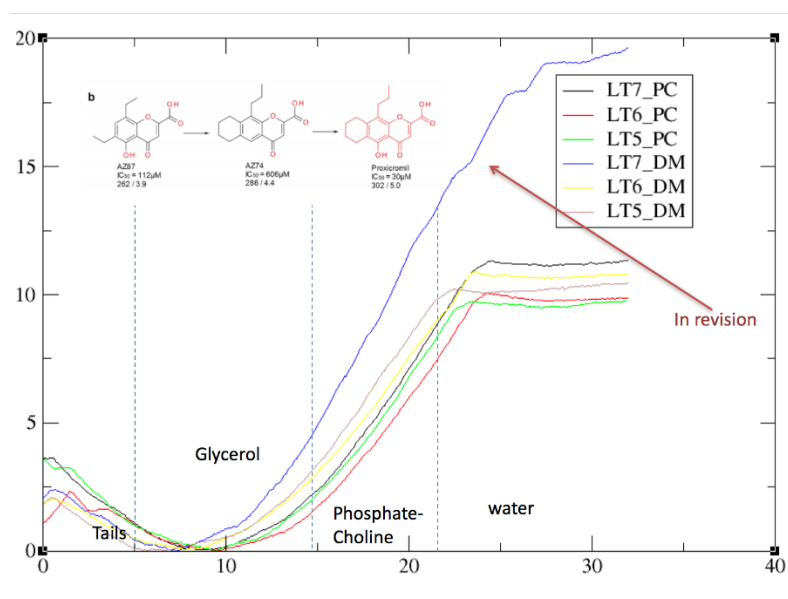


Figure 7: PMF profiles of insertion of group b) ligands in two different lipids, POPC AND DMPC.

Anthracycline Parameterization and Validation

We have performed extensive parameterization work on the Anthracyclines: Doxo-, Epi-, Ida- and Dauno-rubicin. This has required significant application of high level quantum mechanical calculations.

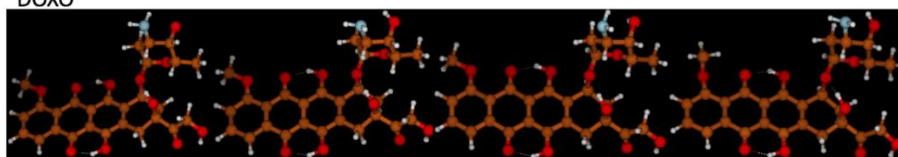
A result is that we now have a set of validated GAFF parameters [22] to facilitate the modelling of the Anthracyclines in lipid bilayers and/or with proteins. We will be able to publish a paper on this process and the level of agreement between our QM and MM results in particular in respect of Raman Spectra.

Method: M06/cc-pvdz

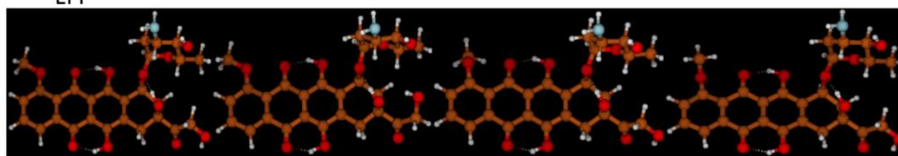
Conformers

	DOXO	EPI	IDA	DNR
Number of Conformers	39	43	11	31

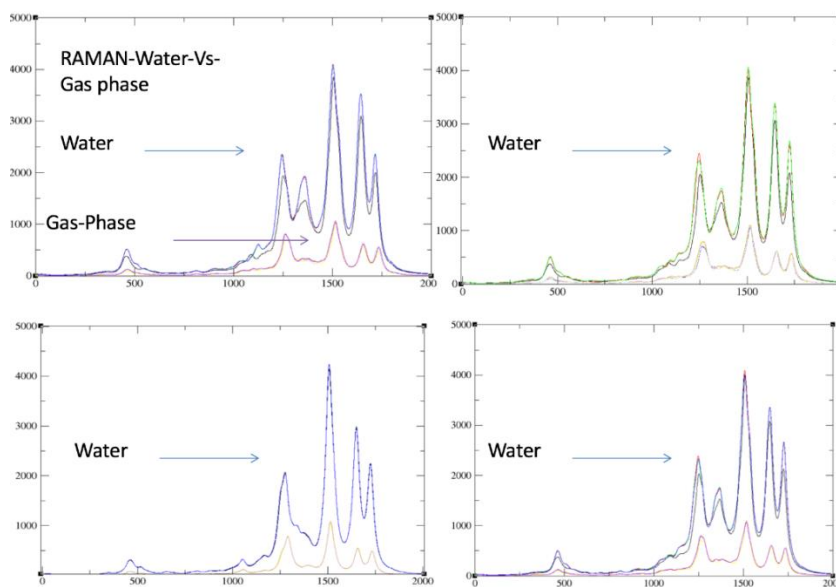
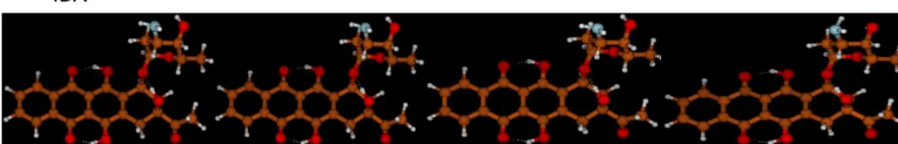
DOXO



EPI



IDA



DIFFICULTIES

The one year gap between Dr Dickson and Dr Toroz starting on the project has meant that we are currently 6 to 12 months behind on this component of the project.

REFERENCES

1. Dickson CJ, Madej BD, Skjevik AA, Betz RM, Teigen K, Gould IR, Walker RC JOURNAL OF CHEMICAL THEORY AND COMPUTATION 10(2):865-879 01
2. Skjevik AA, Madej BD, Dickson CJ, Teigen K, Walker RC, Gould IR, 2015, [All-atom lipid bilayer self-assembly with the AMBER and CHARMM lipid force fields](#), CHEMICAL COMMUNICATIONS, Vol: 51, Pages: 4402-4405, ISSN: 1359-7345
3. Skjevik AA, Madej BD, Dickson CJ, Teigen K, Walker RC, Gould IR, 2016, Simulation of lipid bilayer self-assembly using all-atom lipid force fields. Phys. Chem. Chem. Phys., 2016,18, 10573-10584 . DOI: 10.1039/C5CP07379K
4. Dent MR, Lopez-Duarte I, Dickson CJ, Geoghegan ND, Cooper JM, Gould IR, Krams R, Bull JA, Brooks NJ, Kuimova MK, 2015, [Imaging phase separation in model lipid membranes through the use of BODIPY based molecular rotors](#), PHYSICAL CHEMISTRY CHEMICAL PHYSICS, Vol: 17, Pages: 18393-18402, ISSN: 1463-9076
5. Michael R. Dent, Ismael López-Duarte, Callum J. Dickson, Phoom Chairatana, Harry L. Anderson, Ian R. Gould, Douglas Wylie, Aurimas Vyšniauskas, Nicholas J. Brooks and Marina K. Kuimova, 2016, Imaging plasma membrane phase behaviour in live cells using a thiophene-based molecular rotor,
6. Accepted for publication in Chem. Comm.
7. Daniel J. Warner, Hongming Chen, Louis-David Cantin, J. Gerry Kenna, Simone Stahl, Clare L. Walker and Tobias Noeske, Drug Metabolism and Disposition December 2012, 40 (12) 2332-2341; DOI: <http://dx.doi.org/10.1124/dmd.112.047068>
8. van Meer, G.; Voelker, D. R.; Feigenson, G. W. Membrane lipids: where they are and how they behave. Nat. Rev. Mol. Cell Biol. 2008, 9 (2), 112–124.
9. Lodish, H.; Berk, A.; Kaiser, C. A.; Scott, M. P.; Bretscher, A.; Ploegh, H.; Matsudaira, P. Molecular Cell Biology, 6th ed.; W. H. Freeman: New York, 2007.
10. Phillips, R.; Ursell, T.; Wiggins, P.; Sens, P. Emerging roles for lipids in shaping membrane-protein function. Nature 2009, 459 (7245), 379–385.
11. Nagle, J. F.; Tristram-Nagle, S. Structure of lipid bilayers. Biochim. Biophys. Acta 2000, 1469 (3), 159–195.
12. Katsaras, J.; Gutberlet, T. Lipid bilayers: Structure and interactions; Springer-Verlag: Berlin, 2001.
13. Tieleman, D. P.; Marrink, S. J.; Berendsen, H. J. A computer perspective of membranes: molecular dynamics studies of lipid bilayer systems. Biochim. Biophys. Acta 1997, 1331, 235–270.
14. Berger, O.; Edholm, O.; Jähnig, F. Molecular dynamics simulations of a fluid bilayer of dipalmitoylphosphatidylcholine at full hydration, constant pressure, and constant temperature. Biophys. J. 1997, 72, 2002–2013.
15. Klauda, J. B.; Venable, R. M.; Freites, J. A.; O'Connor, J. W.; Tobias, D. J.; Mondragon-Ramirez, C.; Vorobyov, I.; MacKerell, A. D.; Pastor, R. W. Update of the CHARMM all-atom additive force field for lipids: Validation on Six lipid types. J. Phys. Chem. B 2010, 114 (23), 7830–7843.
16. Poger, D.; Van Gunsteren, W. F.; Mark, A. E. A new force field for simulating phosphatidylcholine bilayers. J. Comput. Chem. 2010, 31 (6), 1117–1125.
17. Jähnig, F.; Lyubartsev, A. P. Derivation and systematic validation of a refined all-atom force field for phosphatidylcholine lipids. J. Phys. Chem. B 2012, 116 (10), 3164–3179.
18. Marrink, S. J.; Risselada, H. J.; Yefimov, S.; Tieleman, D. P.; de Vries, A. H. The MARTINI force field: Coarse grained model for biomolecular simulations. J. Phys. Chem. B 2007, 111 (27), 7812–7824.
19. Orsi, M.; Essex, J. W. The ELBA force field for coarse-grain modeling of lipid membranes. PLoS One 2011, 6 (12), e28637.
20. Chiu, S.-W.; Pandit, S. A.; Scott, H. L.; Jakobsson, E. An improved united atom force field for simulation of mixed lipid bilayers. J. Phys. Chem. B 2009, 113 (9), 2748–2763.

21. Hornak, V.; Abel, R.; Okur, A.; Strockbine, B.; Roitberg, A.; Simmerling, C. Comparison of multiple Amber force fields and development of improved protein backbone parameters. *Proteins: Struct., Funct., Bioinf.* 2006, 65 (3), 712–725.
22. Kirschner, K.N.; Yongye, A.B.; Tschampel, S.M.; González- Outeiriño, J.; Daniels, C. R.; Foley, B. L.; Woods, R. J. GLYCAM06: A generalizable biomolecular force field. *Carbohydrates. J. Comput. Chem.* 2008, 29 (4), 622–655.
23. Wang, J.; Wolf, R. M.; Caldwell, J. W.; Kollman, P. A.; Case, D. A. Development and testing of a general amber force field. *J. Comput. Chem.* 2004, 25, 1157–1174.
24. M. K. Kuimova, *Phys. Chem. Chem. Phys.*, 2012, 14, 12671–12686.
25. A. G. Lee, *Biochim. Biophys. Acta*, 2004, 1666, 62–87
26. Volkova, M. and R. Russell, 3rd, Anthracycline cardiotoxicity: prevalence, pathogenesis and treatment. *Curr Cardiol Rev*, 2011. 7(4): p. 214-20.